Available online at www.sciencedirect.com
ScienceDirect
International Journal of Pharmaceutics 337 (2007) 316–328
INTERNATIONAL JOURNAL OF PHARMACEUTICS
www.elsevier.com/locate/ijpharm

Pharmaceutical Nanotechnology

Use of avidin/biotin-liposome system for enhanced peritoneal drug delivery in an ovarian cancer model

Cristina L. Zavaleta *, William T. Phillips, Anuradha Soundararajan, Beth A. Goins

Department of Radiology, MSC 7800, University of Texas Health Science Center at San Antonio, 7703 Floyd Curl Drive, San Antonio, TX 78229-3900, USA

Received 17 September 2006; received in revised form 18 December 2006; accepted 3 January 2007
Available online 14 January 2007

Abstract

The goal of this study was to determine the distribution of the avidin/biotin-liposome system in an ovarian cancer xenograft model. Optimal avidin/biotin-liposome injection sequence with enhanced liposome accumulation to the peritoneum was determined. Two weeks after NIH:OVCAR-3 cell inoculation, rats were divided into three groups. Group 1 (B-A) ($n=4$), received an intraperitoneal injection of ^{99m}Tc-blue-biotin-liposomes 30 min before an intraperitoneal injection of avidin. Group 2 (A-B) ($n=4$), received an intraperitoneal injection of avidin 30 min before an intraperitoneal injection of ^{99m}Tc-blue-biotin-liposomes. Group 3 (A-B 2h) ($n=5$), received an intraperitoneal injection of avidin 2 h before an intraperitoneal injection of ^{99m}Tc-blue-biotin-liposomes. Three additional non-tumor nude rats served as controls in each group, and were subjected to the same injection sequences. Scintigraphic imaging commenced at various times post ^{99m}Tc-blue-biotin-liposome injection. After imaging, rats were euthanized at 23 h post-liposome injection for tissue biodistribution. Images showed no apparent difference in liposome distribution between control and tumor animals. Regional uptake analysis at 4 h for tumor rats showed significantly higher lymphatic channel uptake in the A-B 2h group ($p<0.05$) and a trend of increased peritoneal uptake in A-B group. By 22 h, peritoneal and lymphatic channel uptake was similar for all groups. At necropsy, most activity was found in blue-stained omentum, diaphragm, mediastinal and abdominal nodes. Bowel activity was minimal. These results correlate with previous normal rat studies, and demonstrate potential use of this avidin/biotin-liposome system for prolonging drug delivery to the peritoneal cavity and associating lymph nodes in this ovarian cancer xenograft model.

Keywords: Ovarian cancer; Liposomes; Drug delivery; Avidin–biotin system; Nude rats; Small animal imaging

1. Introduction

According to the American Cancer Society, ovarian cancer ranks fourth in cancer deaths among women, accounting for more deaths than any other cancer of the female reproductive system (American Cancer Society Website, 2006). This past year it was estimated that 22,220 new cases of ovarian cancer would be diagnosed in the United States alone, of which 16,210 cases would result in death (American Cancer Society Website, 2006). The death rate for this disease has not changed much in the last 50 years, partly due to the fact that most women are diagnosed only after the cancer cells have spread from the ovary to the peritoneum and lymph nodes that receive lymphatic drainage from the peritoneum. Epithelial carcinoma of the ovary is the most common, accounting for 85–90% of all ovarian malignancies (The National Ovarian Cancer Coalition Web site, 2005). Nearly 1 in 67 women will develop this type of cancer (American Cancer Society Website, 2006). If detected early, it is very treatable. Unfortunately, most women with the disease are either asymptomatic, or the symptoms are mistaken for menopausal ailments or intestinal illnesses in its early stages.

There are three distinct methods of metastasis for ovarian neoplasm. The two less common processes are through the blood or lymphatic system. Once in the bloodstream or lymphatic system, the cancer cells can travel and form new tumors in other parts of the body. The most common method of metastasis for ovarian cancer is exfoliation or shedding. In this method, ovarian cancer cells can break away from the ovary and spread to other tissues and organs. When ovarian cancer cells shed, they tend to form new tumors in the peritoneum (National Cancer Institute Web site, 2005). Intraperitoneal seeding is commonly found on the omentum, liver capsule, paracolic gutters, and diaphragm

* Corresponding author. Tel.: +1 210 365 7448; fax: +1 210 567 5549.
E-mail address: czavalet@stanford.edu (C.L. Zavaleta).

0378-5173/$ – see front matter © 2007 Elsevier B.V. All rights reserved.
doi:10.1016/j.ijpharm.2007.01.010

(Woodward et al., 2004). Local reoccurrences on the surface of the peritoneum are also common following initial treatment. This pattern of metastasis and disease reoccurrence has generated significant interest in delivering drugs and therapeutic radionuclides directly into the peritoneum (de Bree et al., 2002; Markman, 2001; Gadducci et al., 2005; Cannistra, 2006).

Many scientists believe that intraperitoneal delivery of drugs and therapeutic radionuclides is the best way to increase their localization to the metastatic cancer (de Bree et al., 2002; Markman, 2003; Schneider, 1994). An intraperitoneal injection can increase either the local drug concentration or the duration of drug exposure to cancer cells within the peritoneum while decreasing systemic drug toxicity.

Some intraperitoneal therapeutic techniques have already resulted in some success. Radiocolloids, such as chromic phosphate, injected intraperitoneally have shown therapeutic effectiveness (Gadducci et al., 2005; Varia et al., 2003; Young et al., 2003). The treatment consists of a therapeutic radionuclide, chromic phosphate, P-32, in the form of a colloidal particle on the order of 600–2000 nm. These particles are relatively large and do not move from the peritoneum and tend to cause bowel toxicity. As a result, metastatic cancer cells within the lymph nodes will not be exposed to the therapeutic P-32 radionuclide.

Intraperitoneally administered chemotherapeutic agents have shown encouraging results for the treatment of ovarian cancer, and investigators in the field of ovarian cancer research have recommended that intraperitoneal delivery be further pursued as a legitimate area of research (Berek et al., 1999; Kaye, 2001). A recent report from the New England Journal of Medicine, has made national headlines describing an increased survival up to 12 months in women with ovarian cancer that received intraperitoneal chemotherapy for advanced stage ovarian cancer (Cannistra, 2006). One problem with this approach is that most drugs administered intraperitoneally are rapidly cleared from the peritoneum. By the end of the intraperitoneal infusion most of the infused drug has passed through the peritoneal lining and into the blood. Little drug remains in the peritoneum and only a minimal amount passes into the lymphatic pathways. The advantages derived from the intraperitoneal injection process seem to be counteracted by the rapid clearance of the drug from the peritoneum.

Intravenously administered pegylated liposomes are now well established as a vehicle to effectively deliver chemotherapeutic agents such as doxorubicin (Doxil^{TM}) with less toxicity and a longer half-life; thus allowing higher amounts of the drug to get to the malignant tissue (Stebbing and Gaya, 2002). Doxil^{TM}, intravenously administered, has proven to be more effective in treating recurrent ovarian cancer than doxorubicin alone due to the increased circulation of the drug (Stebbing and Gaya, 2002). Encapsulating therapeutic agents into liposomes leads to positive differences in systemic distribution, activity, and in the toxicity profile and pharmacokinetics of the drug (Reddy, 2000; Banerjee, 2001). One problem with this intravenous treatment method is that the drug is not targeted to a specific organ. Often, in more advanced cases of ovarian cancer, the lymphatics are also obstructed with tumor cells resulting in the formation of carcinomatous ascites (Feldman, 1975; Feldman et al., 1972). These metastatic cancer cells will remain embedded in the lymph nodes and continue spreading to other areas of the body. Another significant problem with intravenously administered Doxil^{TM} is that it causes significant systemic toxicity. Liposomal doxorubicin administered intraperitoneally has shown great promise in recent studies and was found to be most effective when administered intraperitoneally for carcinoma in the peritoneal cavity (Sadzuka et al., 2002).

The primary objective of this project is to utilize the avidin/biotin-liposome system to prolong the retention of liposomes in the peritoneal cavity and draining lymph nodes in an ovarian cancer xenograft model. This increased retention of liposomes could potentially enhance drug delivery to the ovarian cancer cells that have metastasized to the peritoneal cavity and draining lymph nodes.

The main reason for interest in the avidin/biotin system is the high binding affinity between the two. Avidin is an egg-white derived glycoprotein with an extraordinarily high affinity for biotin, a natural water-soluble vitamin H. Avidin is made up of four identical subunits, and each subunit has a single binding site for biotin (Sakahara and Saga, 1999). Our research group has developed a novel method for retaining intraperitoneally injected liposomes in the peritoneal cavity and associated lymph nodes with the use of this system (Phillips et al., 2000). Liposomes are coated with biotin, which are intraperitoneally injected, followed by an adjacent intraperitoneal injection of avidin. This results in an aggregation of the liposomes, which become entrapped in the peritoneal cavity and in the lymph nodes that drain the peritoneum.

In this article, we extend this basic methodology of peritoneal drug delivery previously reported in Sprague-Dawley rats, to a metastatic ovarian cancer model as a means of prolonging the retention of liposome-encapsulated drugs in the peritoneum while greatly increasing their deposition in lymph nodes that receive lymphatic drainage from the peritoneum. We also studied different intraperitoneal avidin/biotin-liposome injection sequences and injection times to determine which injection protocol provides the best retention of liposomes in the peritoneal cavity. This particular study was conducted with biotin-coated liposomes that encapsulated blue dye and were labeled with technetium-99m (^{99m}Tc), which enabled us to both visualize (invasive) and scintigraphically (non-invasive) identify and quantify liposome distribution. A high-resolution micro single photon emission computed tomography (SPECT)/computed tomography (CT) small animal imaging scanner was used to non-invasively localize the distribution of liposomes after intraperitoneal (IP) administration.

2. Materials and methods

2.1. Preparation and characterization of blue biotin-liposomes

To follow the pharmacokinetics and organ uptake of the avidin/biotin-liposome system with a scintigraphic camera, the biotin-liposomes were labeled with ^{99m}Tc (Phillips et al., 1992).

Before ^{99m}Tc labeling, reduced glutathione (GSH) in PBS, pH 6.3, and patent blue dye were encapsulated in the liposomes. The lipid composition of liposomes includes a phospholipid with biotin conjugated to the head group region (Ogihara-Umeda et al., 1993).

Biotin-coated liposomes were comprised of distearoyl phosphatidylcholine (Avanti Polar Lipids, Pelham, AL)/cholesterol (Calbiochem, San Diego, CA)/*N*-biotinoyl distearoyl phosphoethanolamine (Northern Lipids, Vancouver, Canada)/α-tocopherol (Aldrich, Milwaukee, WI) (58:39:1:2 total lipid molar percentage). Lipid ingredients were co-dried from chloroform (Fisher Scientific, Fair Lawn, NJ) by removing it by rotary evaporation and desiccation for 24 h. The dried lipid film was rehydrated with 300 mM sucrose (Sigma, St. Louis, MO) in sterile water (at a total lipid concentration of 120 μmol/ml), warmed to 55 °C, and then lyophilized overnight. The dried lipid–sucrose mixture was rehydrated with 200 mM GSH (Sigma) in Dulbecco's phosphate buffered saline (PBS) (pH 6.3) and 10 mg/ml patent blue dye (CI 42045; Sigma). Before extrusion, the lipid suspension was diluted to 40 μmol/ml with 100 mM GSH in PBS containing 150 mM sucrose and 10 mg/ml patent blue dye and then extruded through a series of polycarbonate filters (Lipex Extruder, Vancouver, Canada) (2 μm, two passes; 400 nm, two passes; 100 nm, five passes) at 55 °C to form unilamellar liposomes. Unencapsulated GSH, blue dye, and sucrose were then removed by repeated washings and ultracentrifugation at 41,000 rpm for 50 min (Ti 50.2 rotor; Beckman, Fullerton CA). Liposomal pellets were resuspended in PBS containing 300 mM sucrose (pH 6.3) to a total lipid concentration of 60 μmol/ml and stored at 4 °C until needed.

Liposomes were tested for liposomal size by determining the diameter and polydispersity index (PI) using particle size analyzer (Brookhaven Instruments, Holtsville, NY). The PI measures the homogeneity of the liposome sample with regard to diameter. A value of 0.0 determines a completely homogeneous sample while a value of 1.0 determines a completely heterogeneous sample. Liposomes were also tested for phospholipid content by Stewart assay (Stewart, 1980); biotin-phospholipid content by 2-(4′-hydroxyazobenzene) benzoic acid (HABA) assay (Pierce, Rockford, IL); GSH content by BIOXYTECH GSH-400 assay (R&D Systems, Minneapolis, MN); blue dye concentration by spectrophotometry; and sterility and endotoxin levels. GSH, blue dye, and biotin-phospholipid were released from liposomes by detergent solubilization before performing assays. Assays for determining GSH, blue dye, and biotin-phospholipid concentrations were performed using the same methods as described by Medina et al. (2006).

Liposomes were 140 nm (0.057 PI) in diameter and contained 20.3 mmol/l of phospholipid and 2.8 mmol/l GSH. Concentration of blue dye was 1.05 mg/ml. No growth of bacteria was detected and the endotoxin level was >2.5 EU/ml and <5 EU/ml.

2.2. Liposome labeling procedure

Labeling of blue-biotin-liposomes with ^{99m}Tc was performed as described before (Phillips et al., 1992). Briefly, a commercial kit of lipophilic chelator, hexamethylpropyleneamine oxime (HMPAO, Ceretec, GE Healthcare, Arlington Heights, IL), was reconstituted with 5 ml of saline containing 740 MBq (20 mCi) ^{99m}Tc sodium pertechnetate. An aliquot of ^{99m}Tc-HMPAO was added to a suspension of blue-biotin-liposomes (1:1 ratio) encapsulating GSH and incubated at room temperature for 30 min. Free label was removed from the liposomes by passage over Sephadex G-25 column (Amersham Pharmacia Biotech, Uppsala, Sweden). Labeling efficiencies were checked by determining the ^{99m}Tc activity before and after column separation of ^{99m}Tc-blue-biotin-liposomes using a dose calibrator (Atomlab 100 Biodex Medical Systems, Shirley, New York). The labeling efficiency in all the experiments was between 70 and 80%.

2.3. Animal model

An NIH:OVCAR-3 cell line from the ATCC (Manassas, VA) was grown and maintained in a 37 °C incubator under 5% CO_2 and 95% air. The cell line was maintained in ATCC complete growth medium: RPMI 1640 medium with 2 mM L-glutamine adjusted to contain 1.5 g/l sodium bicarbonate, 4.5 g/l glucose, 10 mM HEPES, and 1.0 mM sodium pyruvate and supplemented with 0.01 mg/ml bovine insulin, and 20% fetal bovine serum (American Type Culture Collection Web site, 2004). Penicillin (100 U/ml) and streptomycin (100 μg/ml) antibiotics were also added to decrease possibility of contamination (Gawronska et al., 2002). The cells were harvested before passage 7 and stained with trypan blue dye for viability and counting. After adjustment for cell number, the cells were collected and mixed with saline.

Animal experiments were performed under the National Institutes of Health Animal Care and Use guidelines and were approved by our Institutional Animal Care Committee. A total of 13 female athymic (nu/nu) rats with a mean weight of 155 g were each intraperitoneally injected with 36 million NIH:OVCAR-3 cells in 2 ml of saline (Lecuru et al., 2001), in the right lower peritoneal quadrant using a 23 gauge needle.

2.4. MicroPET imaging

A random group of rats were selected to undergo microPET imaging 1 week before the initial avidin/biotin-liposome experiment in order to validate the presence of ovarian cancer cells in the peritoneal cavity. The rats were fasted for approximately 10 h before imaging commenced. On the day of imaging, each rat was anesthetized with 2.5–3% isoflurane (Vedco Inc., St. Joseph, MO) delivered by 100% oxygen as the carrier gas at 2 l/min through an isoflurane vaporizer (Bickford, Wales Center, NY). The rats were then intravenously injected with approximately 11.1 MBq (300 μCi) of fluorine18-fluorodeoxyglucose (^{18}F-FDG) prepared in house in 0.2 ml of saline using a 25 gauge butterfly needle placed in the tail vein to act as a catheter (to avoid infiltration). Thirty to forty minutes was allowed after the injection for uptake of the radiotracer. During this time the rats were kept warm with a heat lamp and heating pad. The rats were placed prone on the microPET bed with a heating source and imaged with a Rodent R4 MicroPET system manufactured by CTI Concorde Microsystems (Knoxville, TN). Tomographic

images were acquired of the peritoneal cavity for 30 min per rat. The images were then reconstructed and analyzed on IDL Virtual Machine, distributed through Research Systems Inc. and AsiPRO software supplied with the microPET.

2.5. Avidin/^{99m}Tc-biotin-liposome injection groups

Two weeks post-inoculation, the rats were then randomly divided into three groups. An aliquot (1 ml) of ^{99m}Tc-blue-biotin-liposomes was diluted with 1 ml of saline, and this volume (2 ml; 38.4 mg of phospholipid/kg; 40.7 MBq) was injected in the peritoneal cavity in both experimental and control groups (Fig. 1). The first group (B-A) ($n = 4$) received an intraperitoneal injection (2 ml) of 40.7 MBq (1.1 mCi) of ^{99m}Tc-biotin-liposomes encapsulating blue dye. Thirty minutes later, a 0.3 ml intraperitoneal injection of avidin (5 mg) was given to these same rats. The second group (A-B) ($n = 4$) received a 0.3 ml intraperitoneal injection of avidin (5 mg) first, followed by an intraperitoneal injection (2 ml) of 40.7 MBq (1.1 mCi) of ^{99m}Tc-blue-biotin-liposomes 30 min later. The third group (A-B 2h) ($n = 4$) received a 0.3 ml intraperitoneal injection of avidin (5 mg) first, followed by an intraperitoneal injection (2 ml) of 40.7 MBq (1.1 mCi) of ^{99m}Tc-blue-biotin-liposomes 2 h later. For each group, three additional nude rats served as controls. These rats were not inoculated with cancer cells, but were subjected to the same avidin and biotin-liposomes injection sequences and imaging time points as shown in Fig. 1.

2.6. Imaging studies

On the day of imaging, each rat was anesthetized with 2.5–3% isoflurane (Vedco Inc., St. Joseph, MO) delivered by 100% oxygen as the carrier gas at 2 l/min through an isoflurane vaporizer. Imaging commenced immediately after ^{99m}Tc-blue-biotin-liposome injection (baseline). The rats were placed supine on the micro single photon emission computed tomography (SPECT)/computed tomography (CT) bed and imaged with a dual head X-SPECT® system manufactured by Gamma Medica (Northridge, CA). Five-minute anterior/posterior planar images were acquired using low energy/high resolution parallel hole collimators (140 keV window −10 + 15%), at baseline, 30 min, 1, and 4 h, and 10 min planar images were acquired at 22 h post ^{99m}Tc-blue-biotin-liposome injection. SPECT and CT images were acquired at 4 and 22 h post ^{99m}Tc-blue-biotin-liposome injection. SPECT images were acquired for 15 s per projection at 4 h and 60 s per projection at 22 h for a total of 64 projections around the rat (dual head 32 projections each; 180° rotation). CT images were taken using 80 kVp and 0.280 mA for 256 projections. All SPECT images were reconstructed with Lumagen software supplied with the X-SPECT®, and CT images were

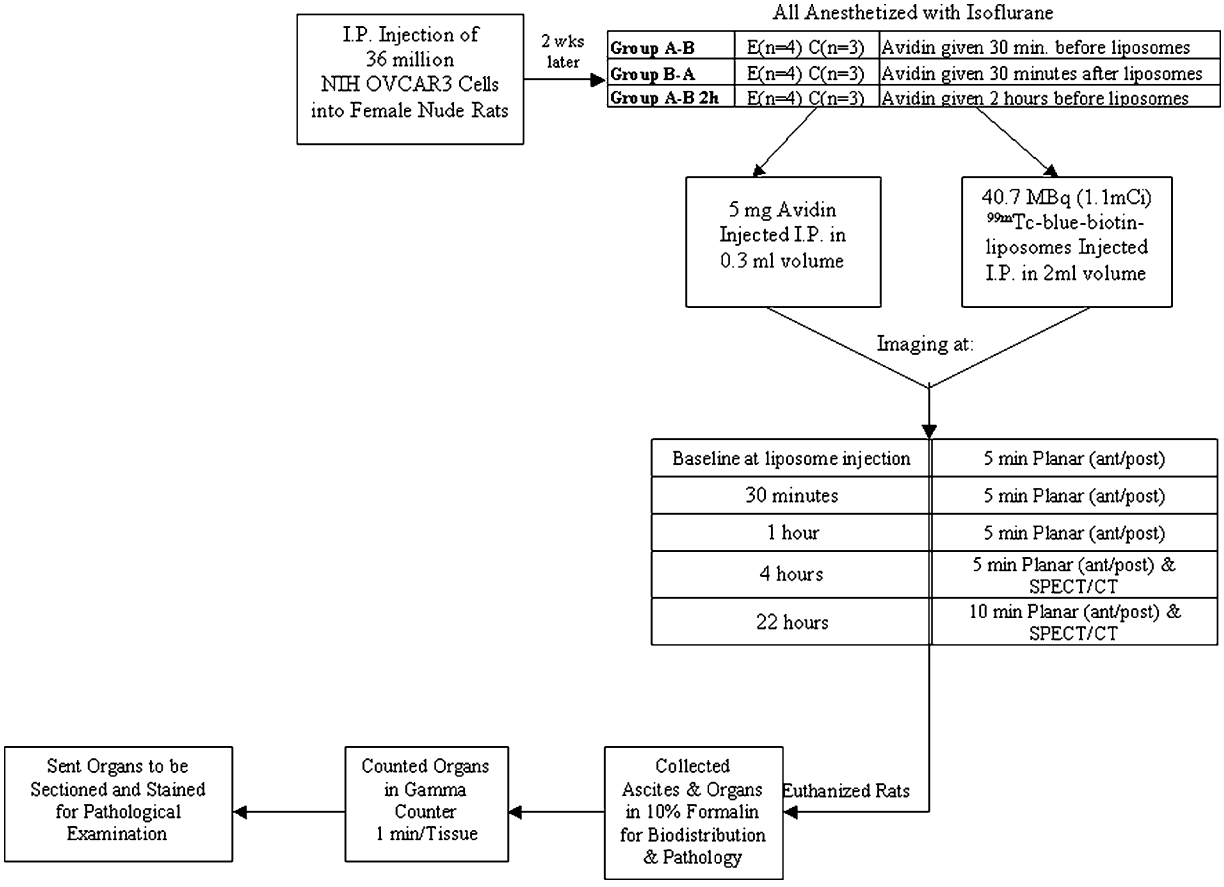

Fig. 1. Schematic representation of the experimental design which shows the sequential timing of the project starting with the intraperitoneal tumor inoculation, followed by the avidin/biotin injection times in the (E) experimental group (tumor) and (C) control group (no tumor), planar and SPECT/CT imaging, and finally organ collection for biodistribution and pathology.

reconstructed using COBRA software. The images were then displayed and analyzed on Amira 3.1.1 distributed through Mercury Computer Systems (Chelmsford, MA).

2.7. Biodistribution

After imaging, the rats were weighed individually to monitor weight loss since tumor cell inoculation. A blood sample (1 ml) was collected via cardiac puncture, while the rats were anesthetized, and placed in a scintillation vial containing 10% formalin for gamma counting. The rats were then euthanized by cervical dislocation under deep isoflurane anesthesia. Ascites were collected in tumor bearing animals using a 3 ml syringe after a small incision was made in the peritoneum and 3 ml of saline was flushed throughout the cavity. The same procedure was performed for collection of normal peritoneal fluid in control animals, for comparison with ascites. Organs were placed in scintillation vials containing 10% formalin and counted approximately 30 h after injection in a Wallac Wizard 3 1480 automatic gamma counter (Perkin-Elmer Life Sciences, Boston, MA). At the time of injection, a standard sample of ^{99m}Tc-blue-biotin liposomes, about 1.11 MBq (30 μCi) in a 30 μl volume, was placed in a microfuge tube and placed on the left side of the rat during planar imaging, the sample was then counted in a scintillation vial and used as a standard reference for tissue biodistribution.

2.8. Standard pathologic examination

To verify the presence of NIH:OVCAR-3 cells, the ascites and peritoneal fluid were smeared onto slides and stained with Giemsa from Sigma–Aldrich (St. Louis, MO) for cytologic examination. Slides were examined with a light microscope.

2.9. Regional uptake analysis

After the planar images were processed, regions of interest (ROI) were drawn around the standard source, lymphatic channels, mediastinal nodes, and peritoneal cavity of each tumor-bearing rat. This data was used to compare the different tumor bearing groups to one another and to quantitatively correlate the images to the biodistribution data. This data was also useful for monitoring liposome accumulation in the lymphatic channels since these tissues were difficult to collect at necropsy. A total activity value based on the intensity of the region was calculated for each ROI using the software supplied with the X-SPECT® and later corrected for individual weight and administered dose to determine the regional uptake using the following formula:

$$\text{regional uptake} = \frac{\text{ROI activity value}}{\text{injected dose/body weight}}$$

The ROI activity value of each tissue was determined by using a standard source of known activity placed in the image field of view. A proportion was set up to calculate the ROI activity value by using the number of counts given for each ROI and its corresponding standard source for each time point.

2.10. Statistical analysis

The data collected from these experiments were analyzed for statistical differences using a 95% confidence interval ($p < 0.05$) using SAS Software (Cary, NC). A Student's *t*-test was used to compare each tumor group to its corresponding control group. Analysis of variance (ANOVA) was used to compare cases where the experimental data contained multiple variables as a function of injection time. The values reported appear as mean ± S.E.M. After statistical analysis was performed using one-way ANOVA, a Duncan's multiple range test was used to compare the individual % ID/g of each tissue of the different tumor groups. The regional uptake data for each tumor group was also statistically analyzed using the same method. A log transformation was applied to the data to better satisfy the assumptions underlying the ANOVA. Means and standard errors were computed from untransformed data and statements of statistical significance were based on transformed data.

3. Results

3.1. Validation of disseminated peritoneal ovarian tumor model

3.1.1. MicroPET imaging

One week post-inoculation, a random selection of rats, later used in this study, were imaged using a microPET camera to confirm the presence of tumor cells within the peritoneal cavity. The radiotracer fluorine 18-fluorodeoxyglucose (^{18}F-FDG) was used, a glucose analog that accumulates in cells with high glucose uptake, particularly cancer cells at the primary tumor site.

The images showed an increased accumulation of ^{18}F-FDG within the peritoneal cavity (Fig. 2). These results are consistent with a previous study we performed where we demonstrated that microPET could be used to non-invasively monitor the development of this particular xenograft model in nude rats (Zavaleta et al., 2005). This pattern of ^{18}F-FDG uptake in the peritoneum indicates that the cancer cells are present in the ascites within the peritoneal cavity.

3.1.2. Cytological examination

Ascites samples were also collected at necropsy and smeared onto slides for microscopic examination, which revealed abundant neoplastic cells with features similar to NIH:OVCAR-3 cells. These results were also consistent with our earlier study in monitoring the development of this tumor model in nude rats (Zavaleta et al., 2005).

3.2. Comparison of avidin/biotin-liposome distribution of tumor bearing rats versus control rats

3.2.1. Imaging

The scintigraphic images revealed no difference in the pattern of ^{99m}Tc-liposome distribution between the tumor bearing and control groups, within each injection sequence (Fig. 3). Control and tumor bearing rats consistently showed the same ^{99m}Tc-

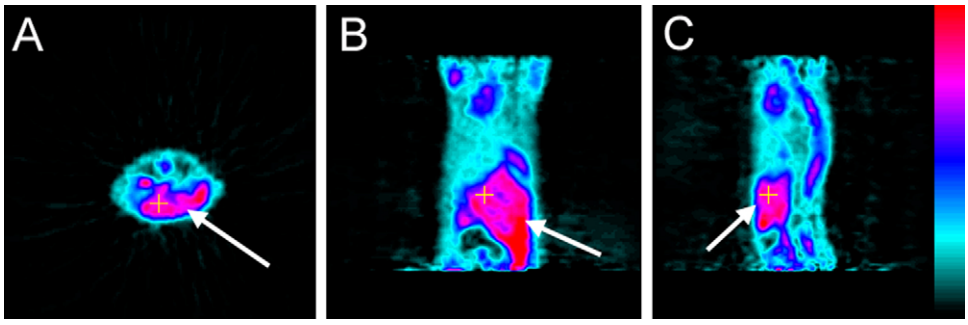

Fig. 2. ^{18}F-FDG microPET images of the peritoneal cavity acquired 30 min post-injection. (A) Transverse slice of peritoneal cavity in tumor bearing rat at 1-week post-inoculation of NIH:OVCAR-3 cells. (B) Corresponding coronal slice of same tumor bearing rat. (C) Corresponding sagittal slice of same tumor bearing rat. The color bar to the right represents the intensity where red is the maximum and black is minimum. Note the intense peritoneal uptake (arrows) of ^{18}F-FDG in these three corresponding slices that represent the accumulation of tumor cells in the ascites of the peritoneal cavity. (For interpretation of the references to color in this figure legend, the reader is referred to the web version of the article.)

liposome accumulation pattern over time within its own injection group. Therefore, the presence of ovarian cancer cells in the peritoneal cavity appears to have no influence on the distribution of liposomes injected intraperitoneally and does not prevent the liposomes from entering the lymphatics and mediastinal nodes.

3.2.2. ^{99m}Tc biodistribution data

The biodistribution of ^{99m}Tc-blue-biotin-liposomes in the control B-A group performed in tumor-bearing immunocompromised nude rats was similar to that reported previously in normal immunocompetent Sprague-Dawley rats (Table 1) (Phillips et al., 2002). The biodistributions from both tumor bearing rats and control rats revealed no statistical difference (Table 1), except for the A-B group (avidin injected 30 min before biotin) with differences between tumor and control rats revealed in the following tissues: abdominal nodes, liver, right ovary, and spleen, all of which displayed increased uptake in the tumor bearing animals. The overall biodistribution data correlates well with the ^{99m}Tc-liposome pattern seen on the scintigraphic images between the tumor and control groups and this distribution provides evidence that the intraperitoneally implanted tumor cells do not alter the normal distribution pattern and uptake levels of these liposomes.

The article will now focus on the characteristics of the liposome injection sequence and how it affects liposome distribution in tumor bearing animals for the remainder of the paper, because future preclinical liposome-based therapies would be tested in this tumor model.

3.3. Liposome accumulation and distribution pattern of tumor-bearing rat groups

3.3.1. Imaging

Planar images revealed a consistent pattern of ^{99m}Tc-liposome retention in the peritoneal cavity and lymph nodes for all three injection groups (B-A, A-B, A-B 2h) of tumor bearing rats (Fig. 3). The images taken at baseline and 1 h post-injection show a similar pattern for all groups where most of the activity is confined to the peritoneal cavity with unique ^{99m}Tc accumulation patterns based on injection sites and physical movement

Table 1
Biodistribution data (%ID/g) of ^{99m}Tc-blue-biotin-liposomes 23 h post-injection

Tissue	Biotin–avidin		Avidin–biotin		Avidin–biotin 2 h	
	Control ($n=3$)	Tumor ($n=4$)	Control ($n=3$)	Tumor ($n=4$)	Control ($n=3$)	Tumor ($n=5$)
Blood	0.090 ± 0.058	0.207 ± 0.182	0.028 ± 0.008	0.034 ± 0.008	0.083 ± 0.016	0.034 ± 0.006
Diaphragm	6.783 ± 1.828	3.532 ± 0.576	8.884 ± 2.413	3.023 ± 0.807	9.674 ± 4.182	8.990 ± 1.382[†]
Heart	0.018 ± 0.007	0.012 ± 0.001	0.016 ± 0.010	0.012 ± 0.002	0.038 ± 0.010	0.022 ± 0.005
Left ovary	1.021 ± 0.988	0.403 ± 0.257	0.083 ± 0.008	0.189 ± 0.070	1.951 ± 1.552	0.920 ± 0.375[‡]
Liver	2.324 ± 0.335	2.807 ± 0.649	0.834 ± 0.541	2.930 ± 0.513[*]	6.380 ± 0.994	3.546 ± 0.682
Mediastinal nodes	15.921 ± 7.203	38.732 ± 17.547	8.047 ± 2.603	18.500 ± 6.461	13.033 ± 2.547	15.442 ± 2.404
Right ovary	1.439 ± 1.404	0.736 ± 0.517	0.074 ± 0.005	0.592 ± 0.283[*]	1.838 ± 0.828	1.333 ± 0.375
Intestines	0.089 ± 0.037	0.112 ± 0.020	0.042 ± 0.004	0.098 ± 0.022	0.229 ± 0.030	0.099 ± 0.010
Cecum	0.155 ± 0.021	0.210 ± 0.035	0.083 ± 0.024	0.139 ± 0.033	0.267 ± 0.057	0.230 ± 0.014
Stomach	0.223 ± 0.038	0.245 ± 0.034	0.145 ± 0.031	0.253 ± 0.074	0.388 ± 0.077	0.220 ± 0.019
Spleen	3.854 ± 0.733	3.541 ± 0.650	1.495 ± 1.012	3.961 ± 1.064[*]	15.038 ± 0.566	6.415 ± 1.121
Abdominal nodes	3.506 ± 1.664	6.918 ± 2.140	3.165 ± 1.002	11.412 ± 2.547[*]	16.651 ± 6.305	12.613 ± 0.975
Omentum	14.381 ± 6.015	21.700 ± 6.112	10.366 ± 0.676	13.139 ± 2.130	12.153 ± 2.682	11.714 ± 1.815

Data are presented as percent injected dose per gram (%ID/g) ± S.E.
[*] Statistically significant with a $p<0.05$ compared with controls of same group.
[†] Statistically significant with a $p<0.05$ compared with other tumor groups of same tissue.
[‡] Statistically significant with a $p<0.05$ compared with avidin–biotin tumor group of same tissue.

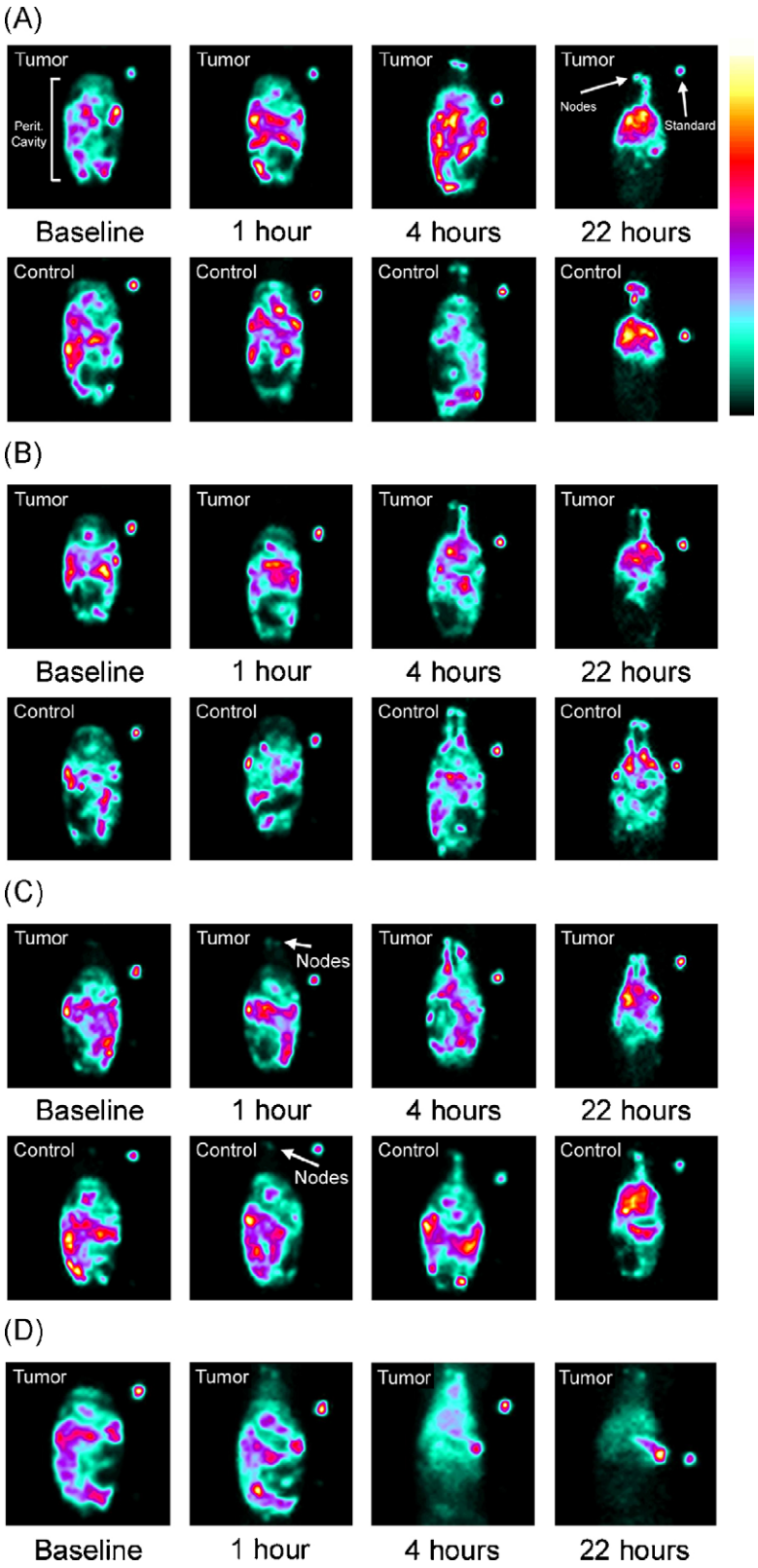

Fig. 3. ^{99m}Tc-biotin-liposome planar images (anterior) of tumor and control animals acquired at baseline, 1, 4, and 22 h post-injection. (A) Group of animals (tumor vs. control) where ^{99m}Tc-biotin-liposomes were injected 30 min before avidin. (B) Group of animals (tumor vs. control) where avidin was injected 30 min before ^{99m}Tc-biotin-liposomes. (C) Group of animals (tumor vs. control) where avidin was injected 2 h before ^{99m}Tc-biotin-liposomes. The color bar to the right represents the intensity where yellow is the maximum and black is minimum. Note the similar distribution pattern between the tumor and control animals within each group. (D) Tumor bearing rat given only ^{99m}Tc-biotin-liposomes without an avidin injection. Notice the rapid clearance of liposomes from the peritoneal cavity as early as 4 h and the intense spleen accumulation at 4 and 22 h, indicating clearance into the blood. (For interpretation of the references to color in this figure legend, the reader is referred to the web version of the article.)

of the rat during consciousness throughout the study. However, in the A-B 2h group, the mediastinal nodes already began to faintly appear in the 1 h images (Fig. 3C) as opposed to the other injection groups (B-A, A-B) where the mediastinal nodes did not appear until the 4 h images (Fig. 3A and B). All groups at the 4 h time point revealed continued retention of ^{99m}Tc-biotin-liposomes in the peritoneal cavity as well as mediastinal node accumulation. The peritoneal activity on the three dimensional SPECT images at 4 h post-injection revealed a very diffuse distribution of ^{99m}Tc-liposomes throughout the cavity (data not shown). In addition, lymphatic channels were seen as early as 4 h in the groups where avidin was injected 30 min and 2 h before the ^{99m}Tc-biotin-liposomes (Fig. 3B and C). In the A-B 2h group, an unusually intense amount of uptake is seen in a pair of lymphatic channels running from the peritoneal cavity to the mediastinal nodes (Fig. 3C). In contrast, lymphatic channel uptake was not evident until 22 h post-injection for the other injection sequence where biotin was injected 30 min before avidin (Fig. 3A). At 22 h, all groups revealed continued mediastinal node uptake as well as peritoneal activity; however, it was difficult to determine from the planar images alone, where exactly the liposomes had accumulated in the cavity. The SPECT/CT fused images gave a better three-dimensional depiction of the distribution throughout the cavity (Fig. 4). Fused SPECT/CT images verified nodal accumulation near the upper sternum as well as increased uptake in the diaphragm at 22 h post-injection.

Fig. 3D is a panel of images taken of a tumor-bearing rat that was given only a ^{99m}Tc-biotin-liposome injection without an adjacent avidin injection. The results correlate well with a previously published paper in normal rats that reports rapid clearance of ^{99m}Tc-biotin-liposomes from the peritoneal cavity and increased spleen accumulation at 24 h post-injection (Phillips et al., 2002). The images shown in Fig. 3D shows increased spleen accumulation as early as 4 h post ^{99m}Tc-biotin-liposome injection. The difference in distribution between the rat given no avidin and the other rats that were given an adjacent avidin injection is readily apparent. ^{99m}Tc-biotin-liposomes are already visible in the mediastinal nodes as early as 1 h post-injection, and the spleen becomes visible as early as 4 h post-injection. By 22 h the mediastinal nodes become faint and most of the activity is seen in the spleen.

3.3.2. Regional uptake analysis

Due to the difficulty of extracting the lymphatic channels at necropsy, biodistribution data was not gathered. Therefore, quantitative analysis of the images was performed to gather more information about the uptake and distribution of ^{99m}Tc-liposomes in these lymphatic channels as well as the mediastinal nodes and peritoneal cavity over the course of 22 h. Fig. 5 shows the average ^{99m}Tc regional uptake data plotted as a function of time. The plots correlated well with the images, which showed a common ^{99m}Tc-biotin-liposome distribution pattern among the groups, where the baseline and 1 h images showed most of the activity confined to the peritoneal cavity. Then at 4 h post ^{99m}Tc-biotin-liposome injection, the lymphatic channels and mediastinal nodes showed increased uptake in addition to peritoneal activity. The data revealed a significant difference in regional uptake in the lymphatic channels at 4 h between the biotin-injected 30 min before avidin group (B-A mean regional uptake = 1.73) and the avidin-injected 2 h before biotin group

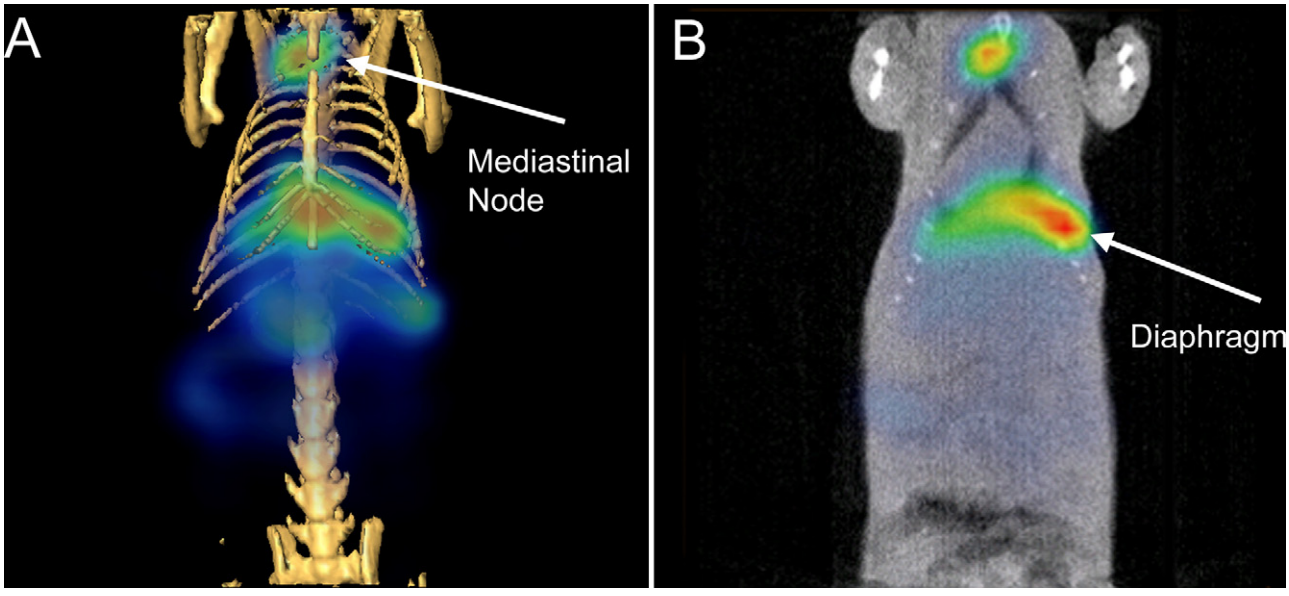

Fig. 4. SPECT/CT fused images of a rat from the A-B 2h group, depicting liposome accumulation at 22 h post ^{99m}Tc-biotin-liposome-injection. (A) Volume rendered CT image using bone window (yellow) superimposed with three-dimensional (3D) SPECT volume (blue to red), showing liposome accumulation in mediastinal nodes near upper sternum and continued peritoneal uptake. Arrow points to increased uptake in mediastinal nodes. (B) Coronal view of CT, set on soft tissue window, and superimposed with SPECT (blue to red) orthoslice depicting liposome accumulation in the diaphragm and mediastinal nodes near upper part of rib cage. Arrow points to increased uptake in diaphragm. These images correlate well with one another and allow anatomical verification (CT) of the increased uptake seen in the 3D SPECT images by overlaying the two sets of images. (For interpretation of the references to color in this figure legend, the reader is referred to the web version of the article.)

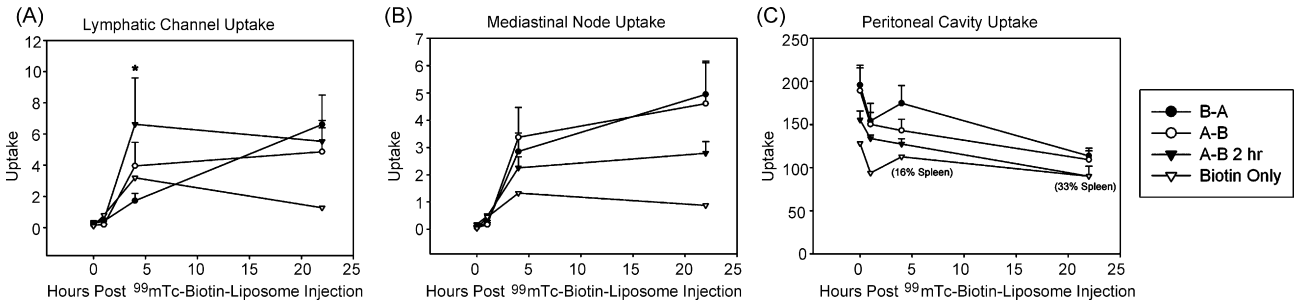

Fig. 5. Average regional uptake data (including standard error of the mean), calculated from regions of interest (ROIs) drawn around the (A) lymphatic channels, (B) mediastinal nodes and (C) peritoneal cavity in tumor bearing animals, plotted over time shows the distribution of liposomes for the different avidin/biotin-liposome injection times over a 22 h period. Notice the difference in liposome accumulation between the groups given biotin-liposomes with avidin vs. biotin-liposomes given alone. *A-B 2h group statistically different from B-A group with a $p < 0.05$, one-way ANOVA.

(A-B 2h mean regional uptake = 6.62) (Fig. 5). Also note the trend that exists in the peritoneal cavity at 4 h, where more of the activity is found in the B-A group (mean regional uptake = 175) than in A-B 2h group (mean regional uptake = 127). Finally, at 22 h, the peritoneal cavity activity drops slightly with continued increased uptake in the lymphatic channels and mediastinal nodes.

3.3.3. ^{99m}Tc biodistribution

The consistent increased peritoneal uptake seen on the planar images throughout all the groups at 22 h, and blue staining observed in the tissues mentioned above correlates well with the ^{99m}Tc activity measured in these tissues. The biodistribution results (%ID/g) indicated high amounts of uptake in the blue stained diaphragm, mediastinal nodes, abdominal nodes,

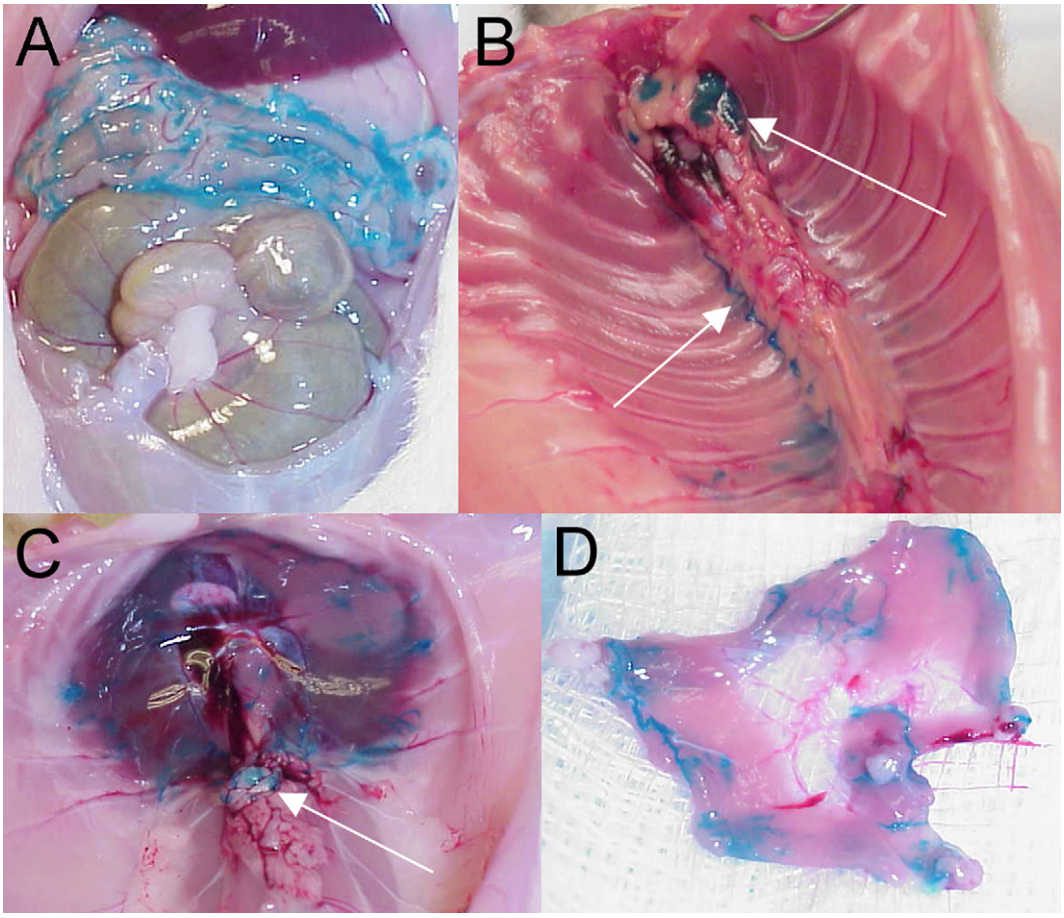

Fig. 6. Gross anatomical images, showing accumulation of ^{99m}Tc-blue-biotin-liposomes in various blue-stained tissues at necropsy. (A) Digital image of the blue stained omentum in the peritoneal cavity. (B) Digital image of blue stained mediastinal nodes and lymphatic channel running along the spine. (C) Digital image of blue stained diaphragm intact. The arrow points to a cluster of blue stained abdominal nodes. (D) Digital image of excised blue stained diaphragm. All groups showed the same staining pattern, although the intensity of the blue staining varied along the lymphatic channels and diaphragm among the different injection groups as discussed within the text. (For interpretation of the references to color in this figure legend, the reader is referred to the web version of the article.)

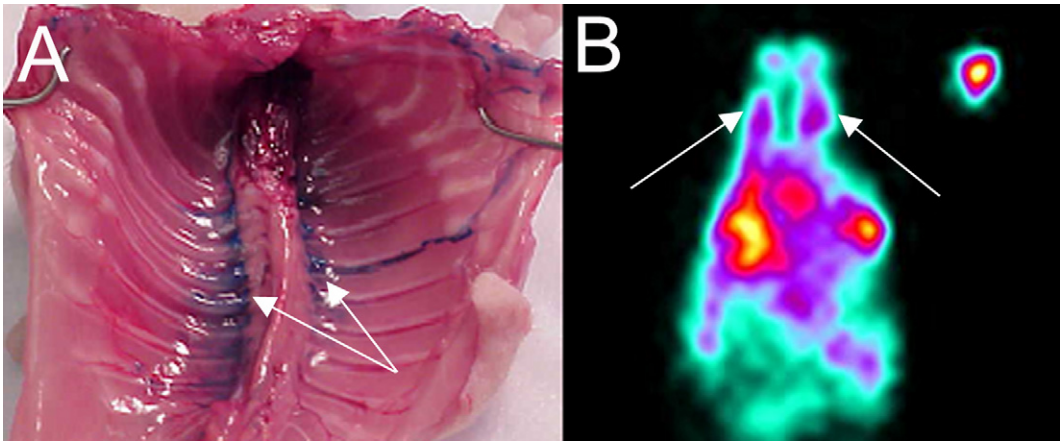

Fig. 7. ^{99m}Tc-blue-biotin-liposome planar image at 22 h shows a strong correlation of liposome accumulation with the gross anatomical image taken of this rat from the A-B 2h group at necropsy. (A) Digital image of the lymphatic channels during tissue collection. The arrows point to the blue stained lymphatic channels running along both sides of the spine. (B) Corresponding planar image that depicts increased uptake of ^{99m}Tc-blue-biotin-liposomes in the same area. The arrows point to the lymphatic channel uptake seen moving up to the mediastinal nodes from the peritoneal cavity. Notice on the planar image how you can resolve each of the lymphatic channels on either side of the spine. (For interpretation of the references to color in this figure legend, the reader is referred to the web version of the article.)

and omentum. Liver and spleen uptake (%ID/g) was minimal in comparison (Table 1). It is apparent that the accumulation seen on the 22 h images in the peritoneal cavity is due to more than just a large liver, but a combination of omentum, diaphragm, and abdominal nodes. Since all of these tissues are in the same overlapping area as the liver, their contribution to the image cannot be resolved by imaging alone. Overall, the %ID/g values were similar for each of the injection sequences as seen in Table 1. However, the %ID/g in the diaphragm of the group where avidin was injected 2 h before ^{99m}Tc-biotin-liposomes (A-B 2h = 8.99%) was significantly higher than in the other groups (B-A = 3.53%, A-B = 3.02%) (Table 1). The % ID/g was also significantly higher in the left ovary of this group (A-B 2h = 0.920%) in comparison with the A-B group (A-B = 0.07%), which correlates with the blue staining seen on the ovaries at necropsy. Blood activity was negligible in all groups, indicating little clearance of ^{99m}Tc-blue-biotin-liposomes from the peritoneum and associated lymph nodes.

Little accumulation of liposomes was seen in the gastrointestinal organs (intestines, cecum, and stomach) throughout all groups (Table 1). This is important when considering this system for a therapeutic approach as bowel toxicity can be a limiting factor when using various radionuclides.

3.3.4. Blue dye accumulation

After the 22 h imaging time point, the rats were sacrificed for tissue collection. At necropsy, ^{99m}Tc-blue-liposome distribution was visualized by blue dye staining. Blue staining of the omentum, diaphragm, mediastinal and abdominal nodes was clearly demonstrated in all the injection groups (Fig. 6). There was also blue staining along the lymphatic channels running near the spine of the rats, which correlates with the 22 h scintigraphic images for all the groups. Blue staining of the lymphatic channels in the A-B 2h group correlated with the planar images; showing two separate blue channels running along either side of the spine (Fig. 7). This blue staining appeared more intense in this group of animals as opposed to the previous groups with only 30 min injection intervals between them. In addition, some blue staining was also found on the ovaries of this group (A-B 2h) of animals. However, the same intensity of blue staining was found throughout all the groups on the other suspecting tissues including: omentum, diaphragm, mediastinal and abdominal nodes. The accumulation of blue dye matched the activity seen on the 22 h planar images, supporting the distribution of the liposomes seen on these images non-invasively.

Table 2 shows the total amount of blue dye, in terms of micrograms, delivered by the liposomes to the blue stained tissues seen at necropsy. The values presented in Table 2 were calculated

Table 2
Total amount of blue dye delivered by liposomes in tissues of interest

Organ	Dose (μg)/organ			Dose (μg)/g tissue		
	B-A (n = 4)	A-B (n = 4)	A-B 2h (n = 5)	B-A (n = 4)	A-B (n = 4)	A-B 2h (n = 5)
Omentum	41.240 ± 10.961	19.755 ± 2.831	19.515 ± 2.850	81.375 ± 22.920	49.271 ± 7.988	43.928 ± 6.806
Diaphragm	5.543 ± 1.106	4.613 ± 1.283	10.860 ± 1.384	13.245 ± 2.160	11.336 ± 3.026	33.713 ± 5.183*
Mediastinal node	7.766 ± 2.085	8.670 ± 2.918	5.539 ± 0.915	145.245 ± 65.801	69.375 ± 24.229	57.908 ± 57.908
Abdominal node	4.016 ± 0.926	4.586 ± 1.954	6.139 ± 0.484	25.943 ± 8.025	42.795 ± 9.551	47.299 ± 3.656

Data are presented as mean ± S.E.M. Based on the %ID/organ data and %ID/g values presented in Table 1.
* Statistically significant with a $p < 0.05$ compared with other tumor groups of same tissue.

from the %ID/organ data and the %ID/g data presented in Table 1 and the total amount of phospholipid and blue dye measured in the blue-biotin-liposomes. Notice how the B-A group shows more blue dye delivered to the omentum than the other injection groups. The A-B 2h group also shows significantly more accumulation of blue dye in the diaphragm.

4. Discussion

As stated earlier, ovarian cancer is the deadliest gynecologic malignancy, with approximately 70% of patients presenting with peritoneal involvement at the time of diagnosis. Common sites of intraperitoneal seeding include the omentum, paracolic gutters, liver capsule, and diaphragm. Stages III and IV are considered advanced, where stage III includes diffuse peritoneal and abdominal involvement and stage IV has distant metastasis to areas outside the peritoneal cavity such as the lymph nodes of the neck (Woodward et al., 2004). Some of the main problems that exist with current intravenous chemotherapy techniques for advanced stage ovarian cancer includes little drug concentration to the peritoneal cavity and rapid drug clearance from the cavity. We have addressed these issues by using an intraperitoneal injection to increase drug concentration to the metastatic cells in the peritoneal cavity, as well as using the aggregating properties of avidin and biotin to retain the liposomes in the peritoneal cavity for a longer period of time. The potential of using this avidin/biotin-liposome system is clear for metastatic ovarian cancer drug delivery. The metastatic cancer within the peritoneum and its associating lymph nodes are prime targets for this system.

The present paper investigated the use of the avidin/biotin-liposome system in tumor bearing rats inoculated with an ovarian cancer cell line. The results showed liposome accumulation and retention in the mediastinal nodes, diaphragm, and omentum for up to 22 h post-injection, where some of the metastatic cancer cells could be located. Secondly, different timing sequences in administering avidin and biotin-liposomes were evaluated in order to determine the best timing for maximum retention in the peritoneal cavity, diaphragm or lymph nodes depending on the tissue of interest. The control group of female nude rats used in this experiment displayed very similar liposome distribution and accumulation patterns to the normal male Sprague-Dawley rats used in the previous paper published using the same injection technique where biotin-liposomes were injected 30 min before avidin (Phillips et al., 2002). These results indicate the lymphatic system clearance mechanism has not been significantly altered in the nude rats (Phillips et al., 2002).

We also tested the results stated in this previous paper (Phillips et al., 2002) that when a rat is given biotin-liposomes alone without an avidin injection, the distribution pattern is quite different. Our results also validate these findings in a tumor-bearing rat. Without an adjacent avidin injection, the biotin-liposomes quickly cleared the peritoneal cavity of the tumor-bearing rat by moving through the lymph nodes and returning to the blood circulation. By 4 h the liposomes had almost completely cleared the cavity and accumulated in the blood, liver and spleen. At 22 h, images and biodistribution results showed massive spleen accumulation (%ID/g = 25.30%), with very little ^{99m}Tc-liposomes in any other organs (Fig. 3D).

Based on the images and biodistribution results, the distribution of the liposomes over time was not altered by the presence of ovarian cancer cells in the peritoneal cavity. Lymphatic obstruction could result in liposome retention in the peritoneum and prevent the liposomes from reaching the lymph nodes, negating the advantages of this delivery system (Phillips et al., 2002). However, in the current study, no apparent obstructions are observed in the lymphatics due to the presence of ovarian cancer cells. Furthermore, due to the time point at which we decided to initiate the study (2 weeks post-inoculation), metastasis to the lymphatics is unlikely (Lecuru et al., 2001). Our cancer model was intended to mimic more of a diffuse metastatic lesion to the peritoneal cavity or a stage III environment, since this is what most women present with at the time of diagnosis (Woodward et al., 2004).

Only minimal differences were found between the distributions of liposomes when using different avidin/biotin-liposome injection times. However, there was a significant difference in liposome accumulation in the lymphatic channels at 4 h between the A-B 2h group and the B-A group. We believe this may be attributed to the highly positive charge that exists on the avidin (Goldman et al., 2002). Since the avidin was injected 2 h before the biotin-liposomes, it had time to enter the lymphatics and attach to the naturally negatively charged lymphatic tissue. When the biotin-liposomes were injected, they aggregated and accumulated in the lymphatic channels earlier (1 h post-injection) instead of passing straight through to the mediastinal nodes, and remaining there for a longer period of time.

There was also a significant difference between the injection groups in the uptake of the ^{99m}Tc-biotin-liposomes in the diaphragm. The uptake was significantly higher in the A-B 2h group than the B-A and A-B groups. Again, this result is likely because the avidin had more time to accumulate around the diaphragm, so that when the ^{99m}Tc-biotin-liposomes were injected they would aggregate in the same area. Blue staining of the diaphragm was also more intense for the A-B 2h animals, which correlates with the biodistribution data. The pattern of blue staining around the diaphragm also suggests that it may be the entry point to the lymphatic channels leading to the mediastinal nodes (Tsilibary and Wissig, 1987; Abu-Hijleh et al., 1995). This notion correlates well with the higher uptake seen in the lymphatic channels of the A-B 2h animals.

There also appears to be a trend for more peritoneal activity to be observed in the B-A animals than the A-B 2h animals (Fig. 7). This also correlates with the increased ^{99m}Tc activity measured in the omentum of the B-A group (%ID/g = 21.70) as opposed to the A-B 2h group (%ID/g = 11.71). Since the avidin was injected 30 min after the biotin-liposomes, there was not enough time for the avidin to localize in a particular area, such as the lymphatics or diaphragm, and just aggregated in the peritoneal cavity once it had met up with the biotin-liposomes already in the cavity.

Therefore, depending on the area of interest, either peritoneal metastasis (stage III) or distant metastasis (stage IV), would ultimately determine the best injection technique to initiate treatment. Combined fractionated therapy could also be an option

where the first treatment fraction would be with B-A to get more drug localization to the peritoneal cavity, followed by an A-B 2h treatment fraction to increase drug concentration to distant metastasis in the lymphatic channels and mediastinal nodes.

Recent research has shown that investigators have been using antibodies to further localize drugs to the ovarian cancer cells within the peritoneal cavity by using a three-step avidin–biotin targeting approach. Xiao et al described the potential for specific targeting of cancer cells using a three-step method in *in vitro* studies of NIH:OVCAR-3 cells (Xiao et al., 2002). This three step targeting approach involves the use of biotin-coated liposomes to carry a therapeutic radionuclide to the target site (tumor). The *in vivo* situation would first involve an intraperitoneal injection containing unlabeled biotinylated monoclonal antibodies to an ovarian cancer antigen such as the CA-125 antigen. Once the antibodies have been given time to attach to the tumor cells, another intraperitoneal injection would be given containing avidin, which has a high binding affinity to biotin. The avidin bound to the biotin on the monoclonal antibody on the tumor cells will have additional binding sites available allowing for the final intraperitoneal injection of biotin-coated radiolabeled liposomes to attach and treat the tumor locally. Another paper described some encouraging preliminary results for the potential of this multi-step radioimmunotherapeutic approach with liposomes in an ovarian cancer animal model expressing CA-125 antigen (McQuarrie et al., 2005). They concluded that using yttrium-90 (^{90}Y) labeled biotinylated long-circulating liposomes indicated a delay in the onset of tumor and ascites development in treated animals. More recently, another paper has described the potential of this three-step approach, without the use of liposomes, in the role of managing advanced stage ovarian cancer in women (Grana et al., 2004).

As a result of recent interest in molecular imaging, new imaging equipment has been developed to produce high-resolution images solely dedicated to small animal research (Green et al., 2001). Diagnostic imaging can play an important role in developing a new therapeutic cancer technique by utilizing its non-invasive properties. In this study, MicroSPECT/CT served as a useful tool to non-invasively monitor the distribution of liposomes over time, and could prove useful in establishing future treatment studies. The radioactive properties of ^{99m}Tc agent allowed the non-invasive visualization of the distribution of the radiolabeled liposomes throughout the body over time.

The potential problems that could be encountered with the avidin/biotin-liposome system include the immunogenicity of avidin, the selection of an optimal intraperitoneal injection technique for women and drug-related toxicity associated with an intraperitoneal delivery route. Although significant progress to design less immunogenic forms of avidin has been reported (Chinol et al., 1998; Caliceti et al., 2002), more research is needed on developing adequate injection techniques. The baseline images of the rats all show a relatively different pattern of accumulation when the ^{99m}Tc-liposomes were injected first into the peritoneal cavity. A more consistent method of injecting the avidin and biotin-liposomes needs to be developed. Perhaps the use of catheters could ensure appropriate delivery of the agents (Twardowski, 2006). The fact that an intraperitoneal injection in a rat may not be a good representation of how the drugs may distribute in humans also needs to be taken into account. The natural stance of a rat (belly down), and a human (upright) are very different and needs to be considered in the development of this technique. Patients may need to stay in bed for a long period of time or be massaged around the abdominal area to ensure the best drug delivery to the entire peritoneal cavity. A recent paper has shown how scintigraphic imaging of therapeutic radionuclides can non-invasively show the correct localization after intraperitoneal injection in women (Grana et al., 2004). This is of great importance when injecting more than one thing in the peritoneal cavity in order to avoid an intraperitoneal "hot area", a potential risk of local radiotoxicity. Since many therapeutic and diagnostic techniques involve injections of radioactive material into the peritoneal cavity, several models have been developed to determine the dosimetry of intraperitoneally injected radionuclides. These methods could be useful in further development of this system (Watson et al., 1989; Syme et al., 2003). Addressing the issue of bowel toxicity would be of particular interest in further developing this system as it could be a major limitation for radiotherapeutic applications in humans. However, the results from our study have shown minimal liposome accumulation to the areas of the intestine, stomach and cecum throughout all the rat groups (Table 1). Choosing a radionuclide with a shorter range beta particle may also help in avoiding severe bowel toxicity in humans.

This study has demonstrated that the avidin/biotin-liposome system has great potential for prolonging the retention of liposomes in the peritoneal cavity and associated lymph nodes in this ovarian cancer model. Further studies to determine the optimal delivery protocol, potential intraperitoneal delivery-related toxicities and efficacy should be conducted using this technique with chemo/radio-therapeutic loaded liposomes for the treatment of metastatic ovarian cancer.

Acknowledgements

The authors would like to thank Cristina Santoyo and Shivshankar Raidas for their help in setting up the tumor model used in this study; Ricardo Perez, III for acquiring the planar and MicroSPECT/CT images; University of Texas Health Science Center Radiology Department for providing MicroSPECT/CT scanner time; and Dr. Alex McMahan for his assistance with the statistical analysis. Student support for Cristina Zavaleta is gratefully acknowledged through a training grant from the National Institute for Biomedical Imaging and Bioengineering (NIBIB) 1-T32-EB000817-01A1.

References

Abu-Hijleh, M.F., Habbal, O.A., Moqattash, S.T., 1995. The role of the diaphragm in lymphatic absorption from the peritoneal cavity. J. Anat. 186, 453–467.

American Cancer Society Website, 2006. Available from: http://www.cancer.org/docroot/CRI/CRI_2_3x.asp?dt=33 (cited 31 August 2006) (online).

American Type Culture Collection Web site, 2004. Available from: http://www.atcc.org/ (cited 17 February 2004) (online).

Banerjee, R., 2001. Liposomes: applications in medicine. J. Biomater. Appl. 16, 3–21.

Berek, J.S., Bertelsen, K., du Bois, A., Brady, M.F., Carmichael, J., Eisenhauer, E.A., Gore, M., Grenman, S., Hamilton, T.C., Hansen, S.W., Harper, P.G., Horvath, G., Kaye, S.B., Luck, H.J., Lund, B., McGuire, W.P., Neijt, J.P., Ozols, R.F., Parmar, M.K., Piccart-Gebhart, M.J., van Rijswijk, R., Rosenberg, P., Rustin, G.J., Sessa, C., Willemse, P.H., et al., 1999. Advanced epithelial ovarian cancer: 1998 consensus statements. Ann. Oncol. 10, 87–92.

Caliceti, P., Chinol, M., Roldo, M., Veronese, F.M., Semenzato, A., Salmaso, S., Paganelli, G., 2002. Poly(ethylene glycol)-avidin bioconjugates: suitable candidates for tumor pretargeting. J. Control. Rel. 83, 97–108.

Cannistra, S.A., 2006. Intraperitoneal chemotherapy comes of age. New Engl. J. Med. 354, 77–79.

Chinol, M., Casalini, P., Maggiolo, M., Canevari, S., Omodeo, E.S., Caliceti, P., Veronese, F.M., Cremonesi, M., Chiolerio, F., Nardone, E., Siccardi, A.G., Paganelli, G., 1998. Biochemical modifications of avidin improve pharmacokinetics and biodistribution, and reduce immunogenicity. Br. J. Cancer 78, 189–197.

de Bree, E., Witkamp, A.J., Zoetmulder, F.A., 2002. Intraperitoneal chemotherapy for colorectal cancer. J. Surg. Oncol. 79, 46–61.

Feldman, G.B., 1975. Lymphatic obstruction in carcinomatous ascites. Cancer Res. 35, 325–332.

Feldman, G.B., Knapp, R.C., Order, S.E., Hellman, S., 1972. The role of lymphatic obstruction in the formation of ascites in a murine ovarian carcinoma. Cancer Res. 32, 1663–1666.

Gadducci, A., Cosio, S., Conte, P.F., Genazzani, A.R., 2005. Consolidation and maintenance treatments for patients with advanced epithelial ovarian cancer in complete response after first-line chemotherapy: a review of the literature. Crit. Rev. Oncol. Hematol. 55, 153–166.

Gawronska, B., Leuschner, C., Enright, F.M., Hansel, W., 2002. Effects of a lytic peptide conjugated to beta HCG on ovarian cancer: studies in vitro and in vivo. Gynecol. Oncol. 85, 45–52.

Goldman, E.R., Balighian, E.D., Mattoussi, H., Kuno, M.K., Mauro, J.M., Tran, P.T., Anderson, G.P., 2002. Avidin: a natural bridge for quantum dot-antibody conjugates. J. Am. Chem. Soc. 124, 6378–6382.

Grana, C., Bartolomei, M., Handkiewicz, D., Rocca, P., Bodei, L., Colombo, N., Chinol, M., Mangioni, C., Malavasi, F., Paganelli, G., 2004. Radioimmunotherapy in advanced ovarian cancer: is there a role for pre-targeting with (90)Y-biotin? Gynecol. Oncol. 93, 691–698.

Green, M.V., Seidel, J., Vaquero, J.J., Jagoda, E., Lee, I., Eckelman, W.C., 2001. High resolution PET, SPECT and projection imaging in small animals. Comput. Med. Imag. Graph. 25, 79–86.

Kaye, S.B., 2001. Future directions for the management of ovarian cancer. Eur. J. Cancer 37, S19–S23.

Lecuru, F., Guilbaud, N., Agostini, A., Augereau, C., Vilde, F., Taurelle, R., 2001. Description of two new human ovarian carcinoma models in nude rats suitable for laparoscopic experimentation. Surg. Endosc. 15, 1346–1352.

Markman, M., 2001. Intraperitoneal drug delivery of antineoplastics. Drugs 61, 1057–1065.

Markman, M., 2003. Intraperitoneal antineoplastic drug delivery: rationale and results. Lancet Oncol. 4, 277–283.

McQuarrie, S., Mercer, J., Syme, A., Suresh, M., Miller, G., 2005. Preliminary results of nanopharmaceuticals used in the radioimmunotherapy of ovarian cancer. J. Pharm. Pharm. Sci. 7, 29–34.

Medina, L.A., Calixto, S.M., Klipper, R., Li, Y., Phillips, W.T., Goins, B., 2006. Mediastinal node and diaphragmatic targeting after intracavitary injection of avidin/^{99m}Tc-blue-biotin-liposome system. J. Pharm. Sci. 95, 207–224.

National Cancer Institute Web site, 2005. Available from: http://nci.nih.gov/cancertopics/pdq/treatment/ovarianepithelial/Patient/page1 (cited 31 March 2005) (online).

Ogihara-Umeda, I., Sasaki, T., Nishigori, H., 1993. Active removal of radioactivity in the blood circulation using biotin-bearing liposomes and avidin for rapid tumour imaging. Eur. J. Nucl. Med. 20, 170–172.

Phillips, W.T., Rudolph, A.S., Goins, B., Timmons, J.H., Klipper, R., Blumhardt, R., 1992. A simple method for producing a technetium-99m-labeled liposome which is stable in vivo. Int. J. Radiat. Appl. Instrum. B 19, 539–547.

Phillips, W.T., Klipper, R., Goins, B., 2000. Novel method of greatly enhanced delivery of liposomes to lymph nodes. J. Pharmacol. Exp. Ther. 295, 309–313.

Phillips, W.T., Medina, L.A., Klipper, R., Goins, B., 2002. A novel approach for the increased delivery of pharmaceutical agents to peritoneum and associated lymph nodes. J. Pharmacol. Exp. Ther. 303, 11–16.

Reddy, K.R., 2000. Controlled-release, pegylation, liposomal formulations: new mechanisms in the delivery of injectable drugs. Ann. Pharmacother. 34, 915–923.

Sadzuka, Y., Hirama, R., Sonobe, T., 2002. Effects of intraperitoneal administration of liposomes and methods of preparing liposomes for local therapy. Toxicol. Lett. 126, 83–90.

Sakahara, H., Saga, T., 1999. Avidin–biotin system for delivery of diagnostic agents. Adv. Drug Deliv. Rev. 37, 89–101.

Schneider, J.G., 1994. Intraperitoneal chemotherapy. Obstet. Gynecol. Clin. North Am. 21, 195–212.

Stebbing, J., Gaya, A., 2002. Pegylated liposomal doxorubicin (Caelyx) in recurrent ovarian cancer. Cancer Treat. Rev. 28, 121–125.

Stewart, J.C., 1980. Colorimetric determination of phospholipids with ammonium ferrothiocyanate. Anal. Biochem. 104, 10–14.

Syme, A.M., McQuarrie, S.A., Middleton, J.W., Fallone, B.G., 2003. Dosimetric model for intraperitoneal targeted liposomal radioimmunotherapy of ovarian cancer micrometastases. Phys. Med. Biol. 48, 1305–1320.

The National Ovarian Cancer Coalition Web site, 2005. Available from: http://www.ovarian.org/default.asp (cited 11 April 2005) (online).

Tsilibary, E.C., Wissig, S.L., 1987. Light and electron microscope observations of the lymphatic drainage units of the peritoneal cavity of rodents. Am. J. Anat. 180, 195–207.

Twardowski, Z.J., 2006. History of peritoneal access development. Int. J. Artif. Organs 29, 2–40.

Varia, M.A., Stehman, F.B., Bundy, B.N., Benda, J.A., Clarke-Pearson, D.L., Alvarez, R.D., Long, H.J., 2003. Intraperitoneal radioactive phosphorus (^{32}P) versus observation after negative second-look laparotomy for stage III ovarian carcinoma: a randomized trial of the Gynecologic Oncology Group. J. Clin. Oncol. 21, 2849–2855.

Watson, E.E., Stabin, M.G., Davis, J.L., Eckerman, K.F., 1989. A model of the peritoneal cavity for use in internal dosimetry. J. Nucl. Med. 30, 2002–2011.

Woodward, P.J., Hosseinzadeh, K., Saenger, J.S., 2004. From the archives of the AFIP: radiologic staging of ovarian carcinoma with pathologic correlation. Radiographics 24, 225–246.

Xiao, Z., McQuarrie, S.A., Suresh, M.R., Mercer, J.R., Gupta, S., Miller, G.G., 2002. A three-step strategy for targeting drug carriers to human ovarian carcinoma cells in vitro. J. Biotechnol. 94, 171–184.

Young, R.C., Brady, M.F., Nieberg, R.K., Long, H.J., Mayer, A.R., Lentz, S.S., Hurteau, J., Alberts, D.S., 2003. Adjuvant treatment for early ovarian cancer: a randomized phase III trial of intraperitoneal ^{32}P or intravenous cyclophosphamide and cisplatin—a gynecologic oncology group study. J. Clin. Oncol. 21, 4350–4355.

Zavaleta, C.L., Phillips, W.T., Bradley, Y.C., Jerabek, P.A., Goins, B.A., 2005. Use of MicroPET to non-invasively monitor the development of an intraperitoneal ovarian xenograft model in nude rats. J. Nucl. Med. 46, 235.